

Morphology of localised attacks on 304 austenitic stainless steel stressed by constant tensile load

A. ALDERISIO, M. BIANCHI, B. BREVAGLIERI and G. SIGNORELLI, Dip. Chemical Engineering, Materials, Raw Materials and Metallurgy, Faculty of Engineering, University La Sapienza, Rome.

Abstract

Different forms of localised etch appear on solution heat-treated austenitic stainless steel exposed to solutions of $H_2SO_4 + NaCl$ according to the SO_4^{2-}/Cl^- ratio, under well-defined experimental conditions: presence of pre-formed cavities, application of constant load, polarization to a potential in the region of imperfect passivity.

The forms of etch and the effect of the various parameters are discussed.

Riassunto

Morfologia di attacchi localizzati di un acciaio inossidabile austenitico 304 sollecitato a trazione sotto carico costante.

A carico di un acciaio inossidabile austenitico solubilizzato esposto a soluzioni di $H_2SO_4 + NaCl$ si manifestano forme diverse di attacco localizzato a seconda del rapporto SO_4^{2-}/Cl^- , in condizioni sperimentali ben determinate: presenza di cavità preformate, applicazione di un carico costante. Sono discusse le forme dell'attacco e l'influenza dei vari parametri.

Introduction

Various authors have studied the stress corrosion of stainless steels in $H_2SO_4 + NaCl$ at ambient temperature (1-4).

In a research project aimed at characterising the behaviour under stress of austenitic stainless steels, surface treated by different methodologies, phenomena appear partly traceable to those described in the cited reports. Harston and Scully (1) observed under the scanning electron microscope the results of stress corrosion on sheets of solubilised Type 304 steel with different grain sizes, bent to a U-shape and exposed to solutions of SO_4^{2-}/Cl^- the most studied solution being H_2SO_4 5 N + NaCl 0.5 N.

In the specimens in the original state, in the outermost surface layers, an intergranular progress of the crack was observed. This was further modified to transgranular when, after the creation of free surfaces and releasing of the dislocations before piling up on their grain boundaries, a localised plastic deformation arises which favours the attack at different sites on the boundaries. The authors foresee that, in constant load tests, growth of the extent of the plasticised zone can give an attack of growing intensity with propagation of the crack. The hardening considerably increases the rate of attack. Stress corrosion cracking manifests itself in H_2SO_4 5 N when the concentration of Cl^- ions rises to 1 - 2 N or drops to 0.1 N; in which case a marked intergranular attack is observed on the surfaces.

Transgranular fracture is the result of very deep pits or a tunnel; the width is all the greater when the grain is coarser.

Experiments like the foregoing (2) on specimens deformed at ambient temperature have brought about

the observation of stress corrosion cracks which in surfaces are intergranular, but subsequently evolve into transgranular, presenting wide areas of sponge-like corrosion on both sides of the crack, while in specimens deformed at $-196^\circ C$ under load, a selective attack of deformation martensite appears. Studying the microprocesses that intervene in the initial step of stress corrosion of sensitised austenitic stainless steels (4), basic phenomena have been observed similar to those already described, but not immediately relating to this for the different heat treatment, that predispose paths to preferential attack. Newman and others (5) studying stress corrosion in sensitised Type 304 steel exposed to thiosulphate solutions, arrive at the conclusion, inter alia, that intergranular cracking running through a zone containing deformation martensite is probably the most representative of the modes of crack propagation in stage II.

Materials, apparatus, methodology

The chemical composition of the austenitic stainless steel AISI 304, expressed as percentage by weight, is as follows:

| C | Mn | Si | Cr | Ni | Mo | P | S |
|-------|------|------|-------|------|------|-------|------|
| 0.058 | 1.30 | 0.50 | 18.00 | 9.02 | 0.20 | 0.030 | 0.25 |

From round bar, cylindrical specimens were obtained with a useful length of 40 mm and a diameter of 4.2 mm. The testpieces were solubilised at $1050^\circ C$ for 30 min and quenched in water. Afterwards the oxide layer, and the underlying steel layer affected to a thickness of $100 \mu m$ by compositional changes concerning the

matrix by selective chromium oxidation, were removed with coarse abrasive paper. Smoothing was done with dry silicon carbide paper down to n. 600.

Electrochemical tests were run in stagnant H_2SO_4 0.5 M + NaCl 0.1/0.2/0.3/0.5M at ambient temperature; potentials were determined, related to the saturated calomel electrode (s.c.e.).

Cyclic polarisation curves were plotted to determine the protection potential, E_p , and the critical breakdown potential, E_R , under a constant tensile load of 216 N/mm².

The greater part of the experiment was carried out on prepolarised surfaces at potentials more noble than E_R , under the selected tensile load up to a current density of 10mA/cm² for concentrations of 0.2M Cl⁻ and 30 mA/cm² and held for 3 min at this current density for concentrations of 0.5 M/Cl⁻; the latter up to the formation on the surface of mini-pits with comparable geometry in the various conditions, priming agents in the subsequent polarisation phase at preset potentials.

Finally, polarisations were carried out under constant tensile loads in the field of imperfect passivity, and the surface modifications recorded after variable exposure times.

The adoption of this methodology takes into account what Perkins (6) writes on the importance of the imperfect passivity region when there are already geometric discontinuities, the influence of pits on cracking by stress corrosion or corrosion fatigue is explained by its effect on intensification of the stresses, or on variations in the composition of the centre or its internal potential.

The polarisations were achieved by means of an AMEL potentiostat, Model 549; the potentiodynamic curves were plotted with a scanning rate of 30mV/min.

Results and discussion

On the grounds of the results obtained; it is appropriate to distinguish the tests carried out at a low ratio $\text{SO}_4^{2-}/\text{Cl}^-$ (0.5/0.5) from others at higher ratio.

For a low ratio of $\text{SO}_4^{2-}/\text{Cl}^-$ the imperfect passivity interval is between 200 and 480mV. In the relative tests, the specimens, tensile stressed under a unit load of 216N/mm² and polarised at potentials between 420 and 440mV, after 3h exposure display a strikingly localised corrosion of caving pits, covered by a thin metallic layer and full of flake metal residues. In Fig. 1 the still covered cavities can be distinctly seen (indicated by arrows) and one broken through. Fig. 2

Fig. 1 - Macrograph of a testpiece exposed for 3h to H_2SO_4 0.5N + NaCl 0.5N for 3h. Arrows indicate pits still covered by a thin metallic layer.

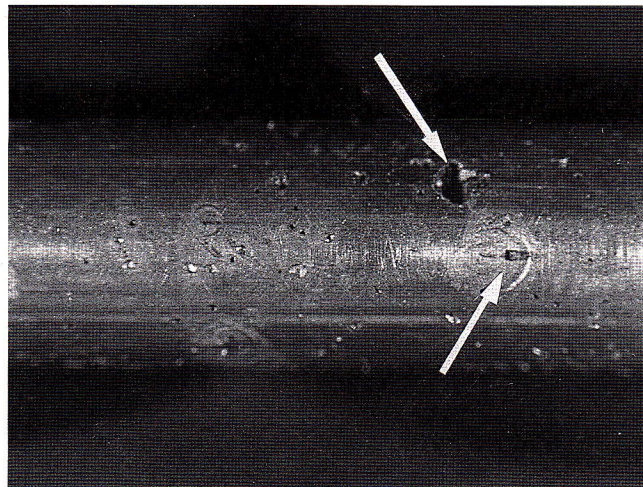
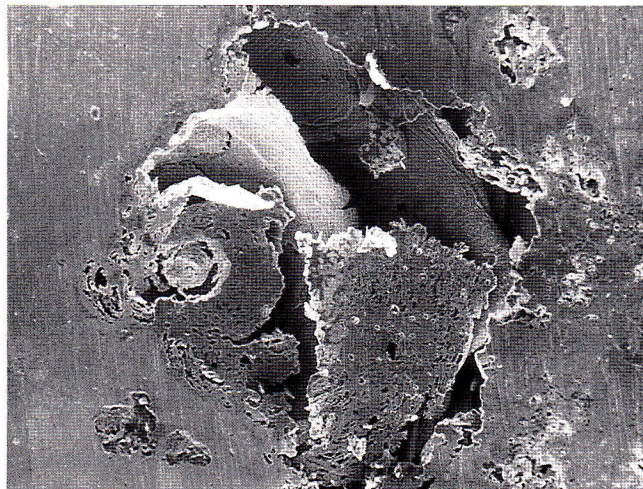


Fig. 2 - SEM micrograph (x 70) of a partially collapsed pit and metal foil residues occurring.



shows details of a pit, partly broken through. The morphology of the phenomenon is very like that observed in the initial step of stress corrosion of austenitic stainless steels sensitised in boiling chloride solutions, in which crevice corrosion is partly remarkable (3). In effect, it is probable that in this case too, inside the pit, crevice corrosion is active, for example that due to the cells setting up for different concentration of metal ions between the inside and the outside.

The phenomenon, observed in the conditions described, is not displayed, either persisting in the imperfect passivity interval and shifted to more active

values of 420mV, also prolonging the exposure to 72h, or if the applied load is removed, or even polarising in the critical range. To this it can be added that experiments run under intermediate loads of 132 and 78 N/mm² gave, in the former case corrosive results of the type described, three times out of five, but never in the latter case. Bearing in mind that with tensile tests run at very low strain rate (0.007 mm/min), for an 18/9 austenitic stainless steel a load limit between elastic and plastic behaviour of 177 N/mm² was determined (7), it seems possible to suggest the hypothesis that a threshold value exists equal to 75% of the aforesaid load limit, below which the phenomenon ceases to show up, or indeed is produced but only with a very long latent time.

In the absence of preformed pits, even if still polarising

Fig. 3 - SEM micrograph (x 700); bottom of a pit affected by intergranular attack

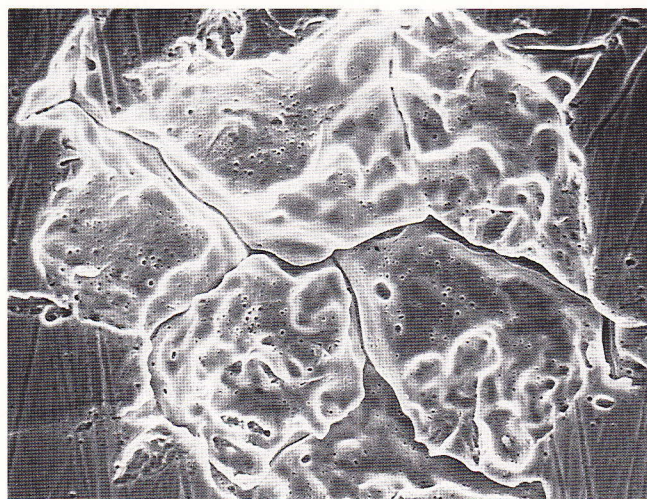
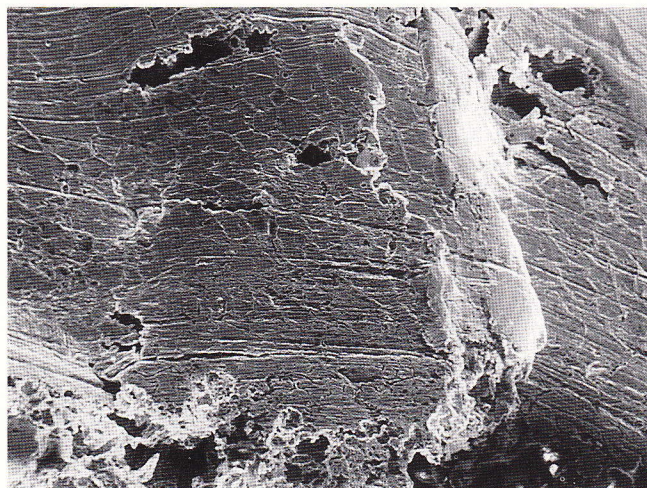


Fig. 4 - SEM micrograph (x 140); side surface of testpiece close to rupture zone. An attack on the microstructure and deformation bands are seen.



in the critical interval and under applied loads, localised corrosion is not observed; this confirms the importance of the geometrical discontinuities already discussed (6).

Tests with higher SO₄²⁻/Cl⁻ ratios were carried out to depress the tendency for Cl⁻ ions to form "caverns". From the course of the polarisation curves and the results of the preliminary polarisation experiments under constant load, it seemed appropriate to concentrate attention on the 0.2M Cl⁻ concentration, this being, for 0.1M the region of the most reduced imperfect passivity, and for 0.3 M an anodic behaviour is similar to that of 0.2 M.

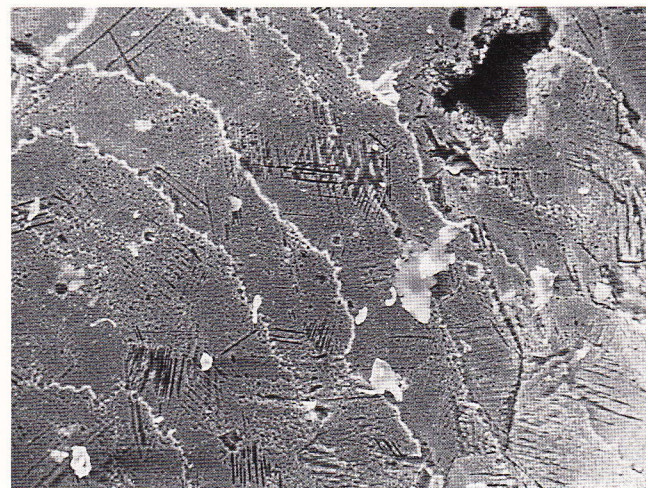
The critical range of polarisation chosen is situated between 850 and 900 mV, being E_R ≈ 940mV and the range of imperfect passivity 250 - 940mV.

After an exposure of 96h at 900mV and under a load of 216 N/mm², at the bottom of the preformed pit an intergranular attack appears, documented in Fig. 3. This attack is not verified either in the test pieces without preformed pits or in those not tensile stressed, or in those polarised at more active potentials than the critical range, as is shown in experiments made at 800mV and extended for a week.

At around 22h a slight initial attack is noted, and for shorter times none at all. Some interesting observations were made on testpieces exposed for 96h to H₂SO₄ 0.5M + NaCl 0.2M, polarised at 900mV, under a load of 216 N/mm² and thinned by the progress of localised corrosion, with diminution of the resisting section, to the point of anticipated rupture. On the side surface, close to the fracture, a light intergranular attack revealed the microstructure Fig. 4).

Examination of the fracture surface by scanning electron microscope shows bands of deformation martensite (Fig. 5) as well as intergranular and

Fig. 5 - SEM micrograph (x 375); bands of deformation martensite.



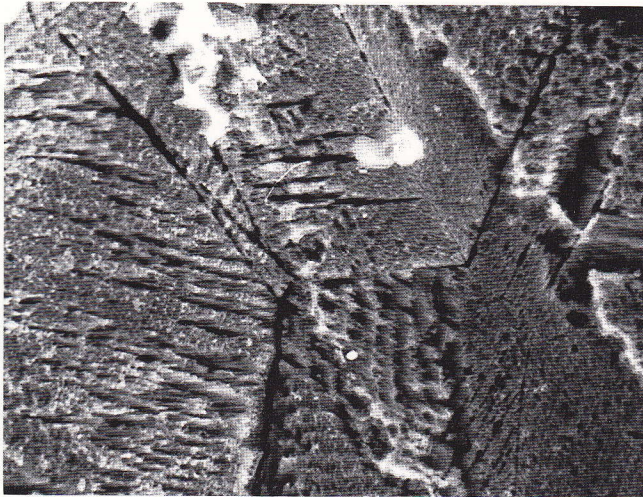


Fig. 6 - SEM micrograph (x 1500); inter- and transgranular attack.

transgranular attack under load, on the aforesaid bands (Fig. 6).

What is observed can be attributed to increase in unit load to values close to that of rupture; this has provoked the appearance of martensite, otherwise absent at ambient temperature.

The phenomena can be classified as selective corrosion under loading of the structure by deformation, as suggested by Hänninen (3).

The deformation structure develops through the following phases: Planar dislocation structure \Rightarrow stacking fault cell structure \Rightarrow ϵ martensite cell \Rightarrow α' martensite.

This last appears in correlation with intersection of the bands of ϵ martensite (3).

Llewellyn and Murray (8) discovered that in a Type 304 steel with a thickness reduction of 12% at ambient temperature, traces of ϵ martensite appear; with 20% you have small amounts of ϵ and α' ; with 30% traces of ϵ remain and small amounts of α' ; with 58% the structure consists of medium/large quantities of γ and medium/small amounts of α' .

The last resulted from the present research, in which polarisation was done in the imperfect passivity region, partially contradicts the thesis that in the passive state there is no appreciable difference between anodic dissolution of the martensite and that of austenite (3).

Conclusions

Results of localised corrosion were observed on specimens of solubilised austenitic stainless steel Type

304, tensile tested under constant load, polarised in the imperfect passivity region.

In H_2SO_4 0.5N + NaCl 0.2N localised corrosion developed, starting from preformed pits, in cavities full of thin flake metal residues.

In H_2SO_4 0.5N + NaCl 0.2N localised corrosion shows itself by an intergranular attack at the bottom of the preformed pits, which remain open and result in an absence of corrosion products.

This last environment seems more promising for attempting to reproduce stress corrosion conditions in solubilised steel, when you try to develop the crack from intergranular to transgranular by means of changes in the following experimental conditions: preformed pits, application of tensile stresses, polarisation and controlled potential, $\text{SO}_4^{2-}/\text{Cl}^-$ ratio.

On the other hand, it seems appropriate to give up experimenting with sensitised steels in which the heat treatment induces preferential routes to localised attack, especially in the active field.

Under all the examined conditions, the phenomena are not produced whenever one of the following conditions pertains: presence of preformed pit; tensile stress above threshold value; polarisation in imperfect passivity region.

Selective corrosion was also observed from deformation-structure and surface intergranular attack when the applied load approaches the rupture value.

REFERENCES

- (1) Harston, J.D., Scully, J.C., *Corrosion*, 25 (12), (1969), 493-501.
- (2) Honkasalo, A., *Corrosion*, 29 (6), (1973), 237-240.
- (3) Hanninen, H.E., *International Metals Reviews* (3), (1979), 85-133.
- (4) Hanninen, H.E., Aho-Mantila, I., *Metals Technology*, 9, (1982), 109-116.
- (5) Newman, R.C., K. Sieradzki, H.S. Isaacs, *Met. Trans. A*, 13 A, (1982), 2015-2026.
- (6) Parkins, R.N., *Metals Technology*, 9, (1982), 122-129.
- (7) Dejardins, D., Daret J., Petit M.C., Pauthe J.J., *Corr. Sci.*, 20, (1980), 177-187.
- (8) Llewellyn, D.T., Murray, J.D., *I.S.I. Special Report*, n. 86, (1964), 197-211.